



MATLAB 기반의 프로그램 BasinVis 2.0을 이용한 분지 모델링: 오스트리아 비엔나 분지의 남부 지역에 대한 사례 연구

이은영^{1,‡} · Michael Wagreich²

¹전남대학교 지구환경과학부

²Department of Geodynamics and Sedimentology, University of Vienna

요 약

분지 해석은 퇴적분지의 형성과 진화를 이해하기 위한 연구 분야로서 여러 종류의 지구과학 자료들을 종합적으로 분석해야 하며, 분지의 시공간적 발달을 입체적으로 구현하기 위해서는 모델링 기술이 적용된다. 분지 해석과 모델링 연구를 위해 2016년 MATLAB 기반의 프로그램 BasinVis 1.0이 공개되었으며 최근에는 새로운 기능과 수정된 사용자 인터페이스를 포함한 BasinVis 2.0이 개발되었다. 이 연구에서는 BasinVis 2.0을 이용한 분지 모델링을 소개하기 위해 비엔나 분지의 남부에서 사례 연구를 수행하였다. 이 연구는 BasinVis 1.0을 이용한 비엔나 분지 중북부의 모델링 연구와 함께 앞으로 수행될 비엔나 분지 전지역의 모델링을 위한 예비 연구로서, 연구 지역의 마이오세 퇴적층과 침강 발달을 시공간적으로 구현하였다. 마이오세 초기의 후반 동안 퇴적과 침강은 북동-남서 방향의 주향이동 단층과 안행성 점완 정단층들을 따라 빠르게 나타난다. 하지만 마이오세 중기부터 후기까지 침강은 급격히 감소한다. 이는 인리형 시스템의 발달에 연관하며, 주향이동 분지의 단기간의 빠른 지구조 침강 패턴과 일치한다. 마이오세 중기의 침강은 주로 주향이동 단층을 따라서 나타나는 반면, 마이오세 중기 후반부터는 북-남 방향의 점완 정단층을 따라 저지대로 퇴적 중심지가 이동되었다. 이는 광역적 고응력장이 북동-남서 방향의 횡인장에서 동-서 방향의 인장으로 변화하는 것과 일치한다. 이 연구에서는 다양한 기능과 기법들이 사례 연구에 적용되었으며, 모델링 결과는 BasinVis 2.0이 분지 모델링 연구에 효과적으로 적용 가능함을 보여준다.

주요어: BasinVis 2.0, 분지 해석, 분지 모델링, 침강, 비엔나 분지

Eun Young Lee and Michael Wagreich, 2018, Basin modelling with a MATLAB-based program, BasinVis 2.0: A case study on the southern Vienna Basin, Austria. Journal of the Geological Society of Korea. v. 54, no. 6, p. 615-630

ABSTRACT: Basin analysis is a research field to understand the formation and evolution of sedimentary basins. This task requires various geoscientific datasets as well as numerical and graphical modelling techniques to synthesize results dimensionally in time and space. For basin analysis and modelling in a comprehensive workflow, BasinVis 1.0 was released as a MATLAB-based program in 2016, and recently the software has been extended to BasinVis 2.0, with new functions and revised user-interface. As a case study, this work analyses the southern Vienna Basin and visualizes the sedimentation setting and subsidence evolution to introduce the basin modelling functions of BasinVis 2.0. This is a preliminary study for a basin-scale modelling of the Vienna Basin, together with our previous studies using BasinVis 1.0. In the study area, during the late Early Miocene, sedimentation and subsidence are significant along strike-slip and en-echelon listric normal faults. From the Middle Miocene onwards, however, subsidence decreases abruptly over the area and this situation continues until the Late Miocene. This is related to the development of the pull-apart system and corresponds to the episodic tectonic subsidence in strike-slip basins. The subsidence of the Middle Miocene is confined mainly to areas along the strike-slip faults, while, from the late Middle Miocene, the depocenter shifts to a depression along the N-S trending listric normal faults. This corresponds to the regional paleostress regime transitioning from NE-SW trending transtension to E-W trending extension. This study applies various functions and techniques to this case study, and the modelled results demonstrate that BasinVis 2.0 is effective and applicable to the basin modelling.

Key words: BasinVis 2.0, basin analysis, basin modelling, subsidence, Vienna Basin

(Eun Young Lee, Faculty of Earth System and Environmental Sciences, Chonnam National University, Gwangju 61186, Republic of Korea; Michael Wagreich, Department of Geodynamics and Sedimentology, University of Vienna, Vienna 1090, Austria)

[‡] Corresponding author: +82-62-530-3450, E-mail: eun.y.lee@chonnam.ac.kr

1. Introduction

Sedimentary basins are regions formed due to tectonically induced and prolonged subsidence of the Earth's surface in which sediments accumulate and be preserved for relatively long geological time periods (Einsele, 2000; Miall, 2000; Leeder, 2011; Allen and Allen, 2013). The internal framework of basins results mainly from the interplay between the volume and rate of sediment supply and the rate of generation and spatial distribution of accommodation. The sediment supply depends on the erosion rate and the provenance type and catchment size, and the generation of accommodation is controlled by tectonic subsidence and uplift, global and regional sea-level change, and compaction. To understand the formation and structure of a basin, therefore, all factors influencing on basin evolution should be considered (Lee *et al.*, 2019). Basin modelling is a method to integrate these factors and visualize the basin formation and evolution dimensionally in time and space by applying numerical and graphical techniques. It is of multi-disciplinary nature and often used for hydrocarbon potential and groundwater evaluation.

To allow geoscientists to analyze and visualize basins in a comprehensive workflow within a non-proprietary software environment, BasinVis 1.0 was developed and released as a MATLAB[®]-based modular open-source tool (Lee *et al.*, 2016). BasinVis 1.0 was particularly aimed at quantitative analyses and 2D and 3D visualization of stratigraphic setting and subsidence of basins based on well data and/or stratigraphic profiles. Recently, the program was extended to improve its user-interfaces and add new functions. The upgraded program is designated as Version 2.0. The new functions of BasinVis 2.0 include the estimation of compaction trends and the applications of the refined decompaction techniques, which are examined using porosity and stratigraphic data acquired from Sites U1459 and U1460 of the International

Ocean Discovery Program (IODP). To demonstrate the improved applications of BasinVis 2.0 in basin modelling, this study introduces a case study on the southern part of the Vienna Basin, Austria.

The Vienna Basin is one of the most extensively studied basins by virtue of fundamental geologic research and hydrocarbon exploration over the past 150 years. The Neogene sedimentary succession is documented by numerous boreholes and a dense network of 2D and 3D seismic data, and various aspects of the structural and sedimentary setting of the basin have been analyzed in many publications (e.g., Jiříček and Seifert, 1990; Sauer *et al.*, 1992; Wessely *et al.*, 1993; Kováč *et al.*, 2004; Hinsch *et al.*, 2005; Arzmüller *et al.*, 2006; Strauss *et al.*, 2006; Beidinger and Decker, 2011; Lee and Wagreich, 2016, 2017). The Vienna Basin is located between the Eastern Alps and the Western Carpathians, covering parts of Austria, Slovakia and the Czech Republic in central Europe. However, the basin studies focused mainly on the southern and central parts (Austrian part) of the basin. Recently, in the central and northern parts of the Vienna Basin, crossing the borders of the three countries, a comprehensive study including basin modelling was conducted by Lee and Wagreich (2016, 2017) using BasinVis 1.0. The previously modelled area does not overlap with the area of this study which covers the southern part of the basin. Together with the previous study, this is a preliminary study to prepare for basin-scale evolution modelling of the Vienna Basin.

2. Geologic setting

The Vienna Basin is a Neogene sedimentary basin of about 200 km in length and 55 km in width (Fig. 1), which is subdivided geographically into three parts. The northern part covers the area north of the Kutty graben, and the central part extends from the Kutty graben to the Schwechat depression, including the Zistersdorf depression. The

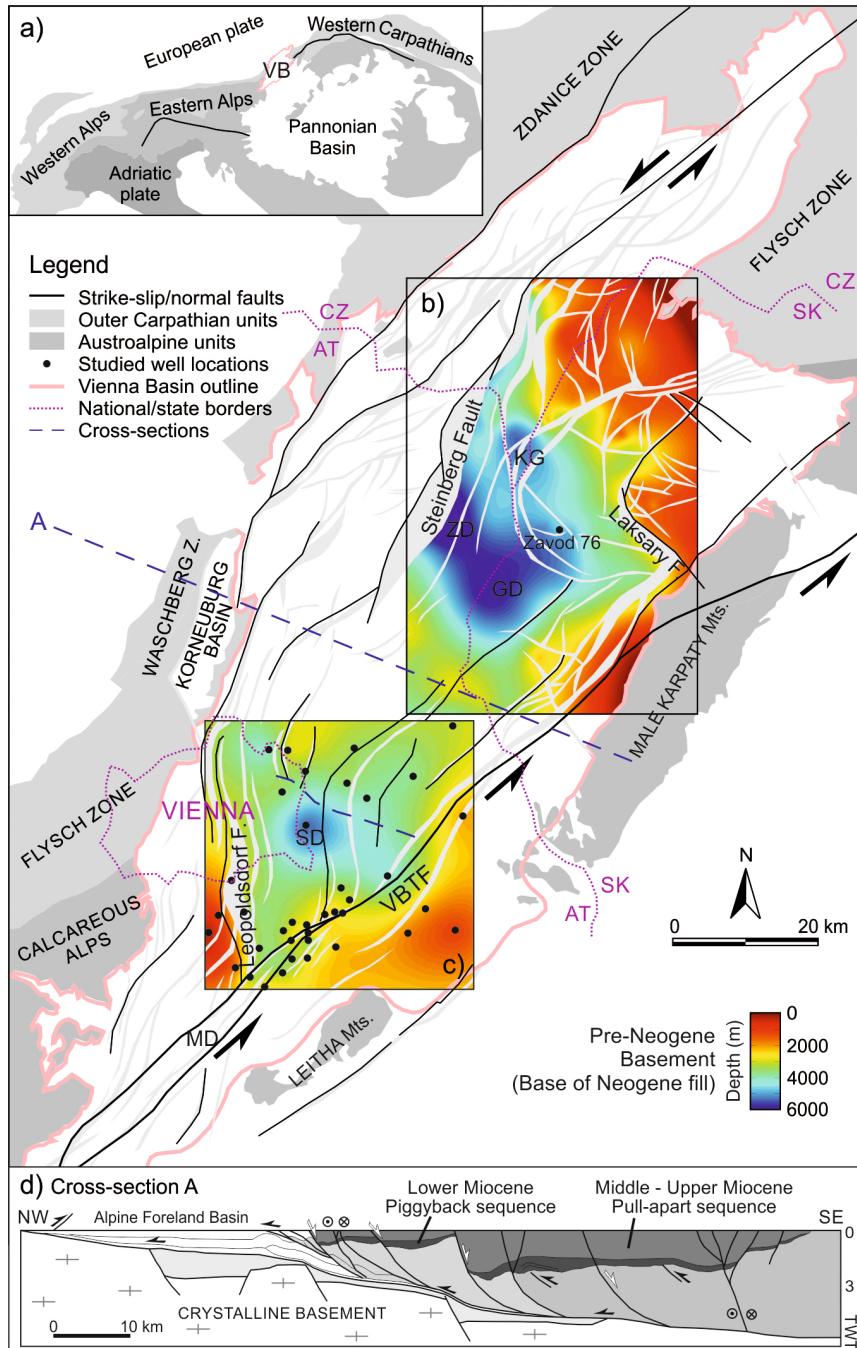


Fig. 1. a) Tectonic sketch map of the east Alpine-west Carpathian region, and the structure map of the Vienna Basin showing the faulted pre-Neogene basement surface and location of cross-section A. AT: Austria, SK: Slovakia, CZ: Czech Republic, VBTF: Vienna Basin transfer fault system, KG: Kutny graben, ZD: Zistersdorf depression, GD: Gajary depression, SD: Schwechat depression, MD: Mitterndorf depression (revised from Wessely *et al.*, 1993; Arzmüller *et al.*, 2006; Lee and Wagreich, 2016). b) Depth map of the pre-Neogene basement (base of Neogene fill) from Lee and Wagreich (2016). Location of well Zavod 76 is shown. c) Study area and depth map of the pre-Neogene basement, the latter being a result of this study. Locations of wells (black dots) are shown. d) Geologic cross-section through the Vienna Basin and the adjacent Alpine Foreland Basin (revised from Beidinger and Decker, 2014).

southern part covers the area of the Schwechat and the Mitterndorf depressions (Lankreijer *et al.*, 1995; Lee and Wagreich, 2017). The Vienna Basin is bordered by the Eastern Alps to the west, the Western Carpathians to the northeast and the Pannonian Basin system to the southeast (Fig. 1a). Due to its position, the Vienna Basin has been influenced by the evolution of each of these geologic systems. The Eastern Alps and the Western Carpathians formed by Alpine-type collisional orogeny during the Mesozoic and the Cenozoic (Royden, 1988; Decker and Peresson, 1996; Plašienka *et al.*, 1997). The late Paleogene and Neogene lateral extrusion of the Eastern Alps towards the Pannonian area in the east caused complex and polyphase strike-slip faulting and back-arc-extension linked to the retreating subduction zone (Ratschbacher *et al.*, 1991a, 1991b). This extrusion further resulted in development of Miocene pull-apart basins (e.g., Vienna Basin) and lithospheric extensional rift basins (e.g., Pannonian Basin) (Mann *et al.*, 1983; Royden *et al.*, 1983a, 1983b; Royden, 1985, 1988; Csontos *et al.*, 1992; Horváth, 1993; Decker and Peresson, 1996; Huismans *et al.*, 2001; Hölzel *et al.*, 2010).

The Vienna Basin is characterized by four distinct tectonic phases (Fig. 2a); 1) Early Miocene piggyback basin, 2) Middle - Late Miocene pull-apart basin, 3) Late Miocene - Pliocene compression and basin inversion, and 4) Quaternary basin formation (Peresson and Decker, 1997a, 1997b; Decker *et al.*, 2005; Strauss *et al.*, 2006; Beidinger and Decker, 2011; Salcher *et al.*, 2012; Lee and Wagreich, 2017).

- 1) In the Early Miocene, several E-W trending small sub-basins (piggyback basins; Ori and Friend, 1984) formed on the frontal parts of the N- to NW-propagating thrust belt of the Eastern Alps. The sediments spread mainly in the northern and central parts of the Vienna Basin (Jiříček and Seifert, 1990; Decker, 1996; Kováč *et al.*, 2004; Strauss *et al.*, 2006; Hölzel *et al.*, 2010).
- 2) At the end of the Early Miocene, the Vienna

Basin became a pull-apart structure due to the lateral extrusion of the Eastern Alps (Fodor, 1995; Decker, 1996). The main tectonic elements are NE-SW trending sinistral strike-slip duplexes and en-echelon listric normal faults (e.g., Steinberg fault, Leopoldsdorf fault, Lassee fault system) with a left-stepping geometry (Royden, 1985, 1988; Decker *et al.*, 2005). Growth strata along normal faults indicate synsedimentary faulting during the Middle Miocene (Decker, 1996; Wagreich and Schmid, 2002; Arzmüller *et al.*, 2006; Strauss *et al.*, 2006).

- 3) In the latest Miocene, the regional stress field switched from N(NW)-directed to E-W-directed compression (Decker and Peresson, 1996; Peresson and Decker, 1997a, 1997b). This phase is characterized by the gradual structural inversion with an uplift of more than 200 m in the Vienna Basin, which caused sediment deformation and erosion (Decker, 1996; Strauss *et al.*, 2006).
- 4) Since c. 250 - 300 ka, the Vienna Basin has been reactivated by NE-SW extension at a releasing bend which is along the slow moving sinistral strike-slip faults and corresponding to the Vienna Basin transfer fault system (VBTF) (Decker *et al.*, 2005; Beidinger and Decker, 2011; Salcher *et al.*, 2012). The small Quaternary basins are developed and filled mainly by fluvial sediments unconformably overlying Miocene sediments (Decker *et al.*, 2005; Hinsch *et al.*, 2005; Salcher *et al.*, 2012).

During the Early Miocene, according to Sauer *et al.* (1992) and Kováč *et al.* (2004), the sediment succession in the north was deposited in a fully marine environment, while the central part of the basin was characterized by deposition of huge freshwater to brackish lacustrine-deltaic formations supplying sediments from the Alps. The southern basin part was fully continental during this time (Fig. 2b). From the Middle Miocene to the Late Miocene, a broad paleo-Danube delta complex on the western

flank of the Vienna Basin carried a massive sediment load from the Alpine Foreland Basin into the Vienna Basin. Small deltaic systems that entered from the southern and northern corners of the basin deposited sediments from areas of the Eastern Alps and the Western Carpathians into

the basin (Sauer *et al.*, 1992) (Fig. 2b).

3. Data and Methods

3.1 Data

The study area covers an area of 37 x 37 km²

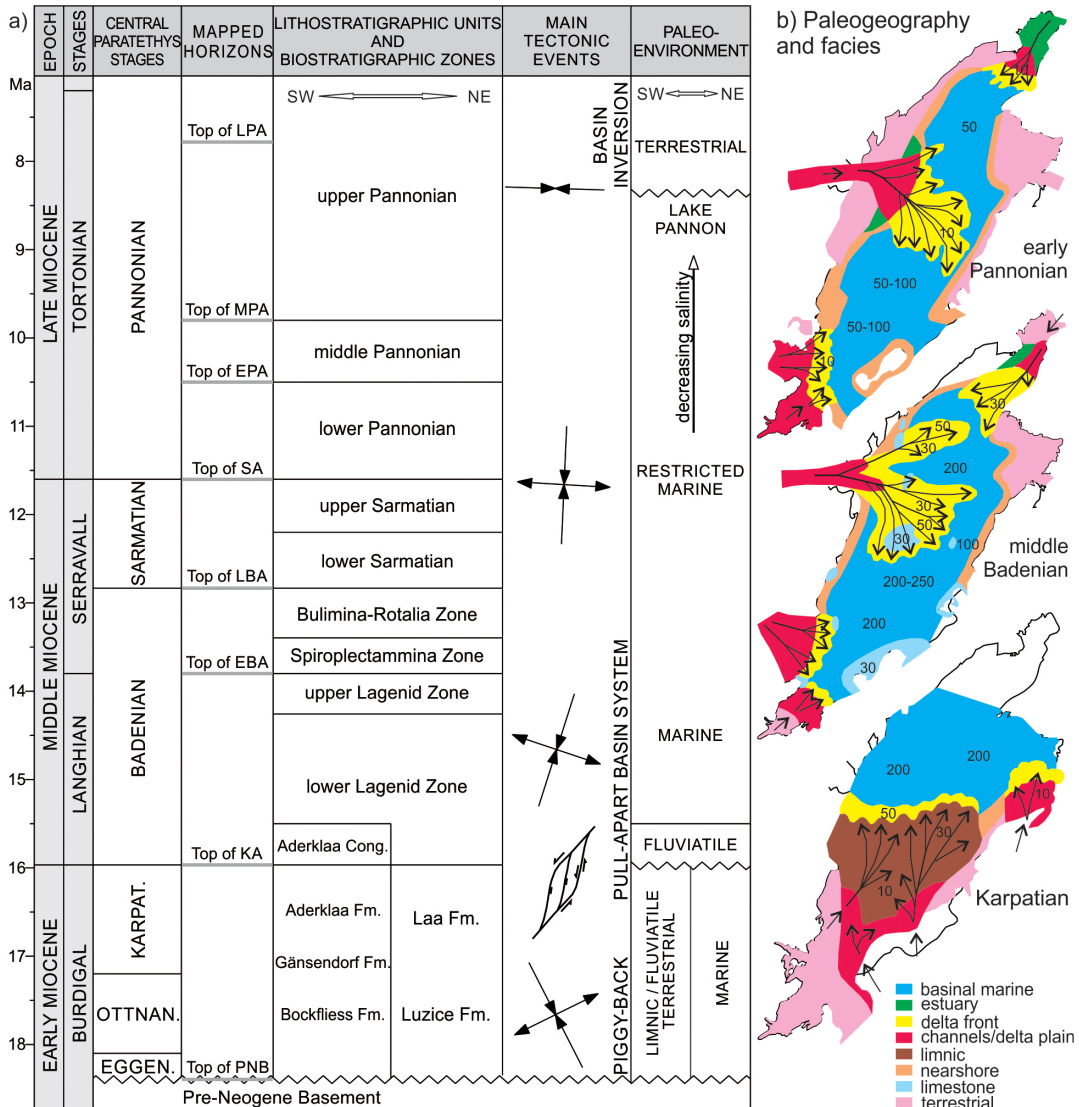


Fig. 2. a) Stratigraphy and evolution of the Vienna Basin in the Miocene (Sauer *et al.*, 1992; Fodor, 1995; Decker, 1996; Peresson and Decker, 1997a; Piller *et al.*, 2007; Hölzel *et al.*, 2010; Hohenegger *et al.*, 2014; Lee and Wagreich, 2016, 2017; Harzhauzer *et al.*, 2018, in press). Horizons mapped in this study area; top of the pre-Neogene basement, top of the Karpatian, top of the early Badenian, top of the late Badenian, top of the Sarmatian, top of the early Pannonian, top of the middle Pannonian, and top of the late Pannonian. b) Paleogeographic and facies models of the Vienna Basin (revised from Sauer *et al.*, 1992); Karpatian, middle Badenian, early Pannonian. Numbers are indicating the paleobathymetry.

in the southern part of the Vienna Basin including the Schwechat depression (Fig. 1c). The sedimentary fill was analyzed using the sediment thickness and stratigraphic data of 38 wells collected from Hölzel (2009) which were provided by OMV E&O Austria. The base depths of the Neogene fill (the depths of the pre-Neogene basement) in the wells were supplemented by using data from the published maps of the Vienna Basin (e.g., Wessely *et al.*, 1993). Because the Alps-Carpathians-Pannonian system was influenced by the Central Paratethys from Oligocene to Miocene times, which was a partly enclosed sea to the north of the Alpine mountain belt, this study uses the regional Central Paratethys chronostratigraphy and regional and local zonations for the Vienna Basin (Piller *et al.*, 2007; Hohenegger *et al.*, 2014; Harzhauser *et al.*, 2018, in press). The well data were arranged for seven successive time steps (Fig. 2a); a) Karpatian (c. 17.2 - 15.97 Ma), b) early Badenian (c. 15.97 - 13.82 Ma), c) late Badenian (c. 13.82 - 12.83 Ma), d) Sarmatian (c. 12.83 - 11.62 Ma), e) early Pannonian (c. 11.62 - 10.5 Ma), f) middle Pannonian (c. 10.5 - 9.8 Ma), g) late Pannonian (c. 9.8 - 7.8 Ma). In the studied well data, the boundary between the late Karpatian and the underlying piggyback sediments is unclear. However, because the study area has thin deposition of lower Karpatian and only sparse

deposition during Otnangian - Eggenburgian time (Jiříček and Seifert, 1990; Sauer *et al.*, 1992; Hölzel *et al.*, 2010), the lowermost unit is defined as Karpatian in this study.

3.2 Subsidence analysis

This study provides two subsidence analysis models which are total subsidence as well as tectonic subsidence (Fig. 3a). In a basin evolution study, the total subsidence represents total depth (depth of basement or total thickness of accumulated sediments) of a sedimentary basin through geologic time. It results from the contribution of various factors including tectonics, sedimentary load, paleobathymetric variation and global sea-level change (Allen and Allen, 2013; Lee *et al.*, 2019).

Total subsidence analysis starts with the division of the stratigraphic column for thickness and age range, and then decompacts each compacted sedimentary layer's thickness successively (decompaction technique). The decompaction process is basically the calculation of the thickness of a sedimentary layer at any time and depth in the past using the appropriate compaction trend (Fig. 3b and c). The equation for compaction trend is typically arranged as an exponential porosity decrease with depth (Athy, 1930; Sclater and Christie, 1980; Bond and Kominz, 1984);

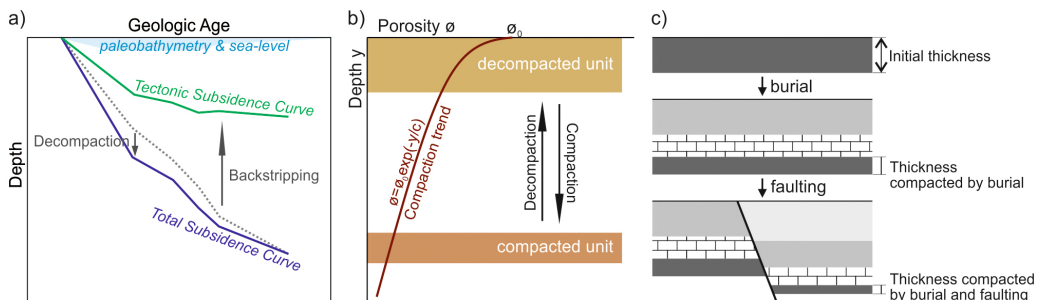


Fig. 3. a) Process of total and tectonic subsidence analysis. Gray dotted line: sediment accumulation curve at present (relative to a fixed datum of paleobathymetry and sea-level variation), blue solid line: total subsidence curve calculated by decompaction technique, green solid line: tectonic subsidence curve calculated by backstripping technique (revised from Lee *et al.*, 2019). b) Concept of compaction and decompaction processes of a stratigraphic unit with exponential compaction trend and equation (revised from Lee *et al.*, 2019). c) Schematic model of successive thickness reduction of sedimentary layers compacted by burial and faulting.

$$\phi = \phi_0 \exp(-y/c)$$

where ϕ : porosity at depth y , ϕ_0 : initial porosity when the layer near surface, c : compaction coefficient. The total amount of restored thickness of accumulated layers provides the base for the total subsidence analysis (Lee *et al.*, 2019).

Tectonic subsidence stands for the amount of subsidence induced by the tectonic driving force (Watts and Steckler, 1979). To identify the tectonic component in basin subsidence, tectonic subsidence analysis performs an isostatic balance between a lithospheric column through the sedimentary basin and a column in which the sediment load has been removed and has been replaced with water. This process is called the backstripping technique (Watts and Ryan, 1976), which is a technique for progressively removing the sedimentary load from a sediment accumulation history (total subsidence) and correcting for compaction, paleobathymetry and sea-level change (Fig. 3a). Incorporating the various effects results in the Airy-isostasy compensated 1D tectonic subsidence (Z) at any geologic time t in the past (Steckler and Watts, 1978; Watts and Steckler, 1979; Sclater and Christie, 1980; Bond and Kominz, 1984);

$$Z(t) = S(t) \left(\frac{\rho_m - \rho_s}{\rho_m - \rho_w} \right) + W_d(t) - \Delta_{SL}(t) \left(\frac{\rho_m}{\rho_m - \rho_w} \right)$$

where $S(t)$: sediment layer thickness at any time t evaluated by decompaction, ρ_w , ρ_m and ρ_s : densities of water, mantle and mean sediment, $W_d(t)$: paleobathymetry at any time t , $\Delta_{SL}(t)$: sea-level change at any time t (Lee *et al.*, 2019).

To estimate the appropriate compaction trend in the Vienna Basin, this study evaluated porosity values using seismic velocity data of well Zavod 76 in the Vienna Basin (Fig. 4a). Seismic velocity data of the well were analyzed by recognizable correlations between seismic velocity-density and density-porosity. A relation between seismic velocity and bulk density defined by Gardner *et al.* (1974) is used;

$$\rho = aV_p^{0.25}$$

where ρ : bulk density, V_p : seismic velocity, a : coefficient. The bulk density is a function of the average density of the rock types making up the formation and the relative volumes occupied;

$$\rho = \rho_s(1 - \phi) + \rho_v\phi$$

where ρ_s : average density of rock matrix, ρ_v : average density of fluid in pore space (Allen and Allen, 2013; Lee and Wagreich, 2017). Based on the porosity-depth relation from well Zavod 97, this study estimated the compaction trend using



Fig. 4. a) Compaction trend for the Vienna Basin. Porosity values were evaluated from seismic velocity data at well Zavod 76 (see Figure 1b for location). b) Main menu of BasinVis 2.0 showing four main stages and subsidiary functions. c) Input parameters for this study.

the function of the 'Compaction Trend Estimation' window in BasinVis 2.0;

$$\phi = 40.2 \exp(-y/6096)$$

where ϕ : porosity at depth y , 40.2: initial porosity when the layer near surface, 6096: compaction coefficient (Fig. 4a).

For the tectonic subsidence analysis of the study area, regional paleobathymetric variations were assumed from Sauer *et al.* (1992) (Fig. 2b). This study has not incorporated eustatic sea-level changes in the calculations, since the basin was separated from the world ocean around the early Late Miocene and the regional sea-level changes in the Paratethys were only partially in accordance with global sea-level cycles (Haq *et al.*, 1987; Steininger and Wessely, 1999; Hohenegger *et al.*, 2014; Harzhauser *et al.*, 2018).

3.3 BasinVis 2.0

BasinVis 2.0 is implemented entirely in MATLAB[®] version 9.3 (R2017b) and requires the 'Symbolic Math' and 'Curve Fitting' Toolboxes (Math, Statistics, and Optimization package). By running the 'mainwindow.m' script in the program folder, BasinVis 2.0 is started and opens the main program window (Fig. 4b) as a central hub accessing to all functions and process stages.

In the 'Setup' stage, this study defined the extent of the study area and the stratigraphic unit names and ages (Fig. 4c), and input the stratigraphic information of well data with coordinates relative to the defined study area. In the 'Stratigraphic Visualization' window, this study visualizes 2D and 3D models of basement surface, sediment distribution, isopach and sedimentation rate of each stage. To evaluate realistic sedimentation rate during the time of deposition, sedimentation rate in this study is based on initial thickness of each stage which is decompacted using the compaction trend. In the 'Subsidence' stage, after inputting parame-

ters for subsidence analysis (Fig. 4c), BasinVis 2.0 computes numerical subsidence analysis of individual wells in the study area. The results are interpolated and visualized for 2D and 3D models of total subsidence depth, total subsidence rate, tectonic subsidence depth and tectonic subsidence rate of each stage (Lee *et al.*, 2016).

Because the collected well data are distributed sparsely and irregularly over the study area (38 well sites in $37 \times 37 \text{ km}^2$), this study integrates the data with MATLAB[®] 3D surface plotting functions provided by BasinVis 2.0. An adopted method to reconstruct the surface in the study area is the Ordinary Kriging (OK) spatial interpolation which originated from the field of geostatistics (Li and Heap, 2008). The OK estimator incorporates the covariance structure between known data points to predict the depth at arbitrary surface locations (Cressie, 1988, 1993). Therefore, surfaces reconstructed using OK result in an entirely smooth surface that inter- and extrapolates the data points over the study area.

4. Results

4.1 Visualization of basement structure

The pre-Neogene basement (base of Neogene fill) of the study area is visualized in 3D surface model (Fig. 5a), and it is compared with a structure map of the Vienna Basin (Fig. 5b). In the 3D basement surface model, the arrangement of prominent highs and depressions is recognizable and dissected by NE-SW trending sinistral strike-slip duplexes and en-echelon listric normal faults. The Schwechat depression and Marchfeld depression show relatively deep subsided depocenters, which are bound by fault blocks of the Leopoldsdorf fault, the Markgrafneusiedl fault and the Lassees fault system. However, the Quaternary basins (Mitterndorf Basin, Aderklaa Basin, Obersiebenbrunn Basin and Lassees Basin) located in this study area do not appear on the basement model.

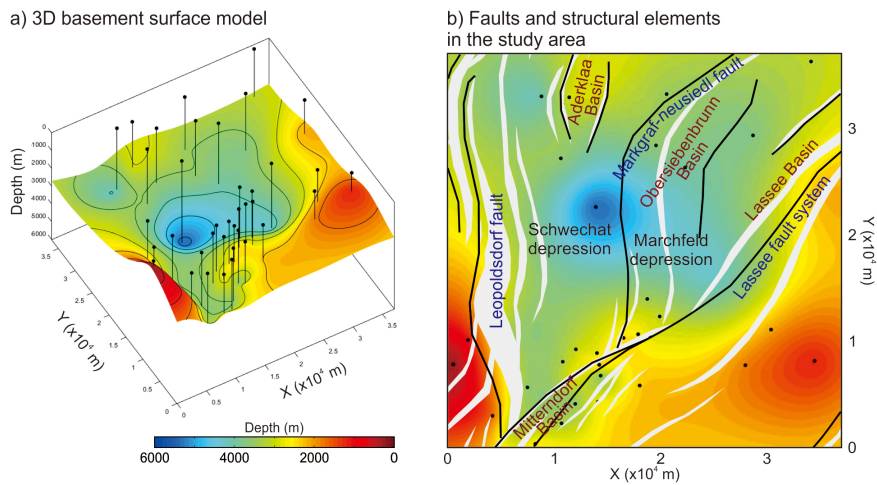


Fig. 5. a) 3D basement (base of Neogene fill) surface model of the study area. b) 2D basement surface model with faults and structural elements. Major faults, depressions and Quaternary basins are labeled. Contour lines (500 m; solid line), well locations (black dots and lines), major faults (bold solid line) and faulted displacement (gray range) are shown.

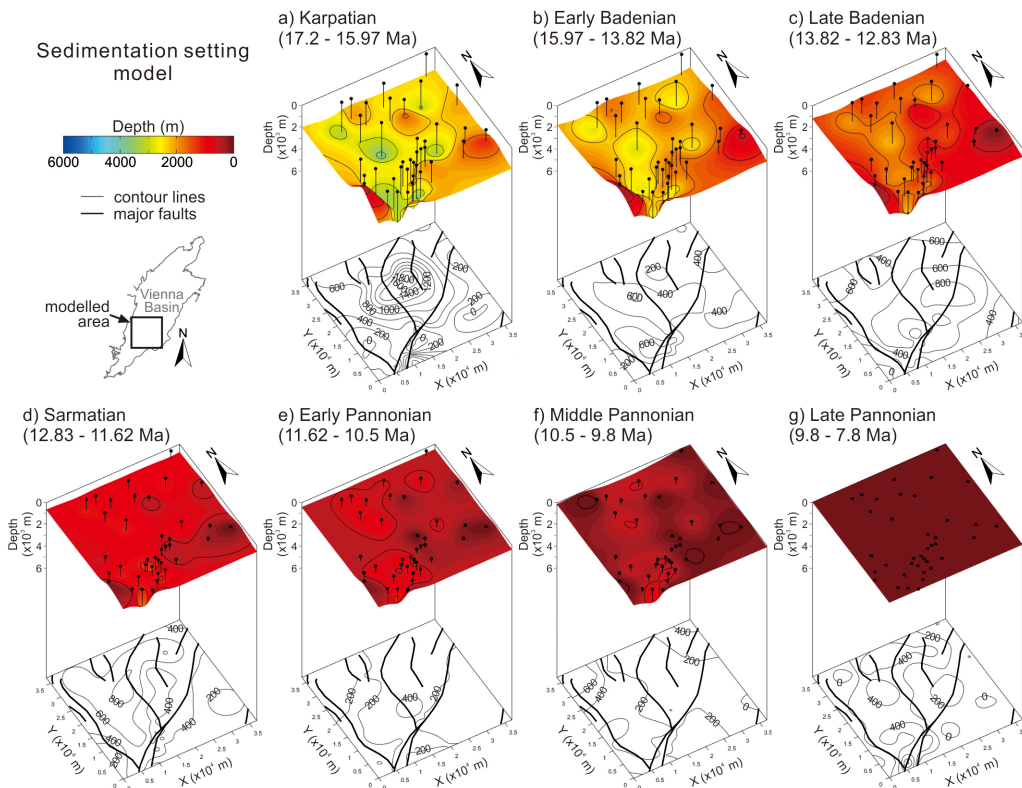


Fig. 6. Sedimentation setting model of the study area. 3D sediment distribution surface (above) and 2D sediment thickness isopach (below) of each stage; a) Karpatian (17.2 - 15.97 Ma), b) early Badenian (15.97 - 13.82 Ma), c) late Badenian (13.82 - 12.83 Ma), d) Sarmatian (12.83 - 11.62 Ma), e) early Pannonian (11.62 - 10.5 Ma), f) middle Pannonian (10.5 - 9.8 Ma), g) late Pannonian (9.8 - 7.8 Ma). Studied wells and contour lines (500 m) are shown in 3D surface models. The major faults and contour lines (200 m) are shown in 2D isopach maps. The top depth of the late Pannonian unit is assumed as 0 m.

4.2 Reconstruction of sedimentation setting

The basin fill of the study area is visualized in 3D sediment distribution surface, 2D isopach map (Fig. 6) and 2D sedimentation rate map (Fig. 7) in seven successive time steps. The isopach maps of sediment thickness show the position of major faults (e.g., Leopoldsdorf fault, Markgrafneusiedl fault, Lasee fault system) to understand the geometrical trend of Miocene sedimentation.

In the Karpatian stage, the overall sediments show a high thickness (up to 1,800 m; Fig. 6a) compared to the other time intervals, with a high sedimentation rate (up to 1600 m/Ma; Fig. 7a). The sediments accumulated mainly along the Markgrafneusiedl fault and Lasee fault system which consists of strike-slip faults and negative flower structures activated along the southwestern margin of the Vienna Basin. The major depocenters are located at/near the Marchfeld depression and Mitterndorf depression. The lower

Badenian sediments are of 200 - 600 m in thickness with a sedimentation rate of around 200 m/Ma (Figs. 6b and 7b). Relatively thick depositional packages are recorded in the Schwechat depression and Mitterndorf depression. During the late Badenian, the sedimentation is NE-SW trending and thick along the Lasee fault system (Fig. 6c). Sedimentation rate is overall 400 - 800 m/Ma in the study area, and a depocenter at the Marchfeld depression shows up to 1,000 m/Ma in sedimentation rate (Fig. 7c). Surface geometries of sediment distribution in the Karpatian - Badenian follow locations and displacement of major fault systems, while the Sarmatian to Pannonian sediments show no indication of fault structure. The Sarmatian sediments attain a varying thickness between 200 - 800 m with a depocenter at the Schwechat depression along the Leopoldsdorf fault (Fig. 6d). The depositional package at the depocenter is 600 - 800 m in thickness with a high sedimentation rate of up to 800

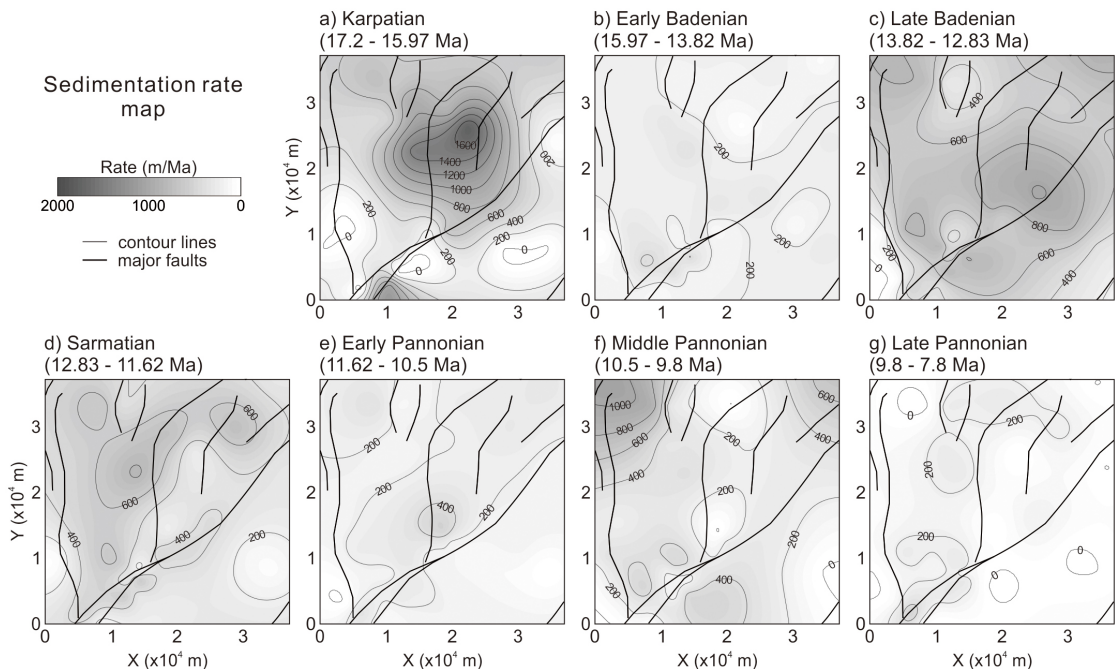


Fig. 7. 2D sedimentation rate map of the study area, based on initial (decompacted) thickness of each stage; a) Karpatian (17.2 - 15.97 Ma), b) early Badenian (15.97 - 13.82 Ma), c) late Badenian (13.82 - 12.83 Ma), d) Sarmatian (12.83 - 11.62 Ma), e) early Pannonian (11.62 - 10.5 Ma), f) middle Pannonian (10.5 - 9.8 Ma), g) late Pannonian (9.8 - 7.8 Ma). The major faults and contour lines (200 m/Ma) are shown.

m/Ma (Fig. 7d). The lower Pannonian sediments are distributed overall with a thickness around 200 m (Fig. 6e) and a sedimentation rate of 200 m/Ma (Fig. 7e). A small depocenter is recorded near the Marchfeld depression. The middle Pannonian sediments attain a varying thickness between 0 - 600 m, and the sedimentation rate is high along the Leopoldsdorf fault but only thin deposits occur at the Mitterndorf depression (Fig. 6f). There are two thicker deposition packages characterized by high sedimentation rates, recorded in the northwestern and northeastern corners of the study area (Fig. 7f). During the late Pannonian, several shallow and small depocenters with ~200 m/Ma in sedimentation rate are distributed in the study area (Figs. 6g and 7g).

4.3 Total and tectonic subsidence model

This study visualizes 3D subsidence depth models and 2D subsidence rate maps of total subsidence and tectonic subsidence at the seven successive time steps (Figs. 8 and 9). The subsidence rate maps show the position of major faults (e.g., Leopoldsdorf fault, Markgrafneusiedl fault, Lassees fault system) to understand the geometrical trend of Miocene subsidence.

Total and tectonic subsidence are considerably fast during the Karpatian, especially along the Markgrafneusiedl and Lassees fault systems (Figs. 8a and 9a). The areas with high subsidence rates (~1,600 m/Ma in total subsidence and ~800 m/Ma in tectonic subsidence) are near/at the Marchfeld depression and the Mitterndorf depression which are bound by the en-echelon fault system and structural ridges consisting of the southwestern transtensional system of the Vienna Basin. After this fast subsidence, both the total and tectonic subsidence decrease markedly during early Badenian time (Figs. 8b and 9b). During the late Badenian, relatively high total and tectonic subsidence commence along the Lassees fault system (600 - 800 m/Ma in total subsidence rate and up to 400 m/Ma in tec-

tonic subsidence rate) showing a NE-SW trend, and also partly along the Leopoldsdorf fault (Figs. 8c and 9c). From the Sarmatian onwards, the subsidence decreases overall in the study area (Figs. 8d and 9d). However, relatively high total and tectonic subsidence rates (400 - 600 m/Ma in total subsidence rate and 150 - 200 m/Ma in tectonic subsidence rate) are indicated in the hanging wall region of the Leopoldsdorf fault and along the Markgrafneusiedl fault. The subsidence during the early Pannonian shows a slight NE-SW trending along the Lassees fault system, and relatively high total subsidence rates (around 200 m/Ma) are recorded at the Mitterndorf depression and the northwestern and northeastern parts of the study area (Figs. 8e and 9e). The northwestern part of the study area subsides significantly during the middle Pannonian (up to 800 m/Ma in total subsidence rate and up to 300 m/Ma in tectonic subsidence rate), which is connected with the Schwechat depression along the Leopoldsdorf fault, while the Marchfeld depression and Mitterndorf depression subside slowly (0 - 200 m/Ma in total subsidence rate and 0 m/Ma in tectonic subsidence rate) during this time (Figs. 8f and 9f). During the late Pannonian, there are no strong subsidence trends or features (Figs. 8g and 9g). Several areas with 200 m/Ma in total subsidence rate are recorded, which partly correspond to the Mitterndorf depression at the southwestern corner of the study area.

5. Discussion

Using functions of BasinVis 2.0, this study visualizes the basement surface, sedimentation setting and subsidence evolution of the study area and analyzes the basin evolution of the Miocene pull-apart structure in the southern part of the Vienna Basin, Austria.

The subsidence during the Karpatian is significant along the Markgrafneusiedl fault and Lassees

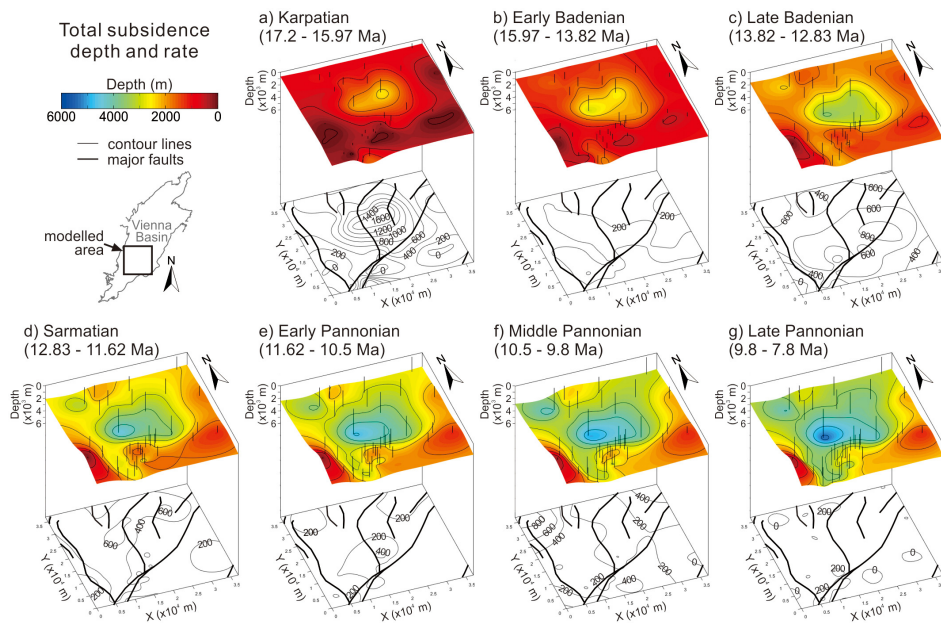


Fig. 8. Total subsidence model of the study area. 3D subsidence depth surface (above) and 2D subsidence rate map (below) of each stage; a) Karpatian (17.2 - 15.97 Ma), b) early Badenian (15.97 - 13.82 Ma), c) late Badenian (13.82 - 12.83 Ma), d) Sarmatian (12.83 - 11.62 Ma), e) early Pannonian (11.62 - 10.5 Ma), f) middle Pannonian (10.5 - 9.8 Ma), g) late Pannonian (9.8 - 7.8 Ma). Studied wells and contour lines (500 m) are shown in 3D depth models. The major faults and contour lines (200 m/Ma) are shown in 2D rate maps.

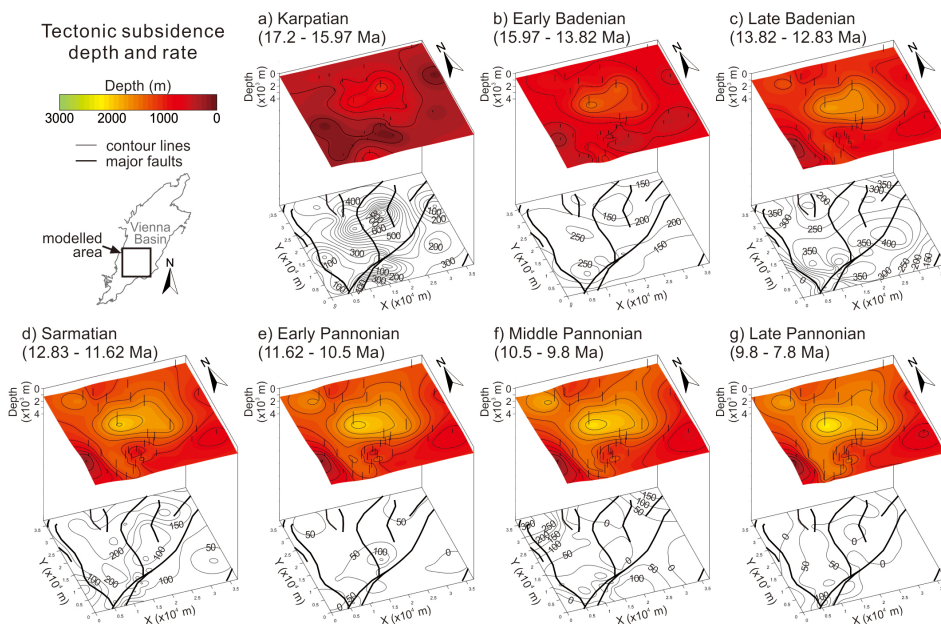


Fig. 9. Tectonic subsidence model of the study area. 3D subsidence depth surface (above) and 2D subsidence rate map (below) of each stage; a) Karpatian (17.2 - 15.97 Ma), b) early Badenian (16.1 - 13.82 Ma), c) late Badenian (13.82 - 12.83 Ma), d) Sarmatian (12.83 - 11.62 Ma), e) early Pannonian (11.62 - 10.5 Ma), f) middle Pannonian (10.5 - 9.8 Ma), g) late Pannonian (9.8 - 7.8 Ma). Studied wells and contour lines (200 m) are shown in 3D depth models. The major faults and contour lines (50 m/Ma) are shown in 2D rate maps.

fault system, which reflects the development of a pull-apart basin system between two left-stepping segments occurred in the Vienna Basin at the end of the Early Miocene (Fig. 10). The faults and structural styles are dominated by NE-SW trending sinistral strike-slip duplexes and en-echelon listric normal faults, and growth strata by synsedimentary faulting are indicated in seismic sections (Strauss *et al.*, 2006; Hölzel *et al.*, 2010; Harzhauser *et al.*, in press).

The subsidence abruptly decreased during the early Badenian and this condition continued until the Late Miocene. This corresponds to the tectonic subsidence patterns of strike-slip basins which are mainly episodic, short-lived (typically <10 Ma) and end abruptly (Xie and Heller, 2009; Lee *et al.*, 2019). The slow subsidence of the early Badenian becomes faster and wider with NE-SW trending along the Lassees fault system. In Hölzel *et al.* (2008), the tectonic subsidence rate of the early Badenian (Upper Ladinid Zone) is higher than the rate of late Badenian in the southern Vienna Basin. However, the tectonic subsidence pattern is not observed in the models of this study. This can result from different methodo-

logical details (e.g., chronostratigraphy, compaction trend, unit boundary).

Different from the largely varying geometries in the sediment surface models of the Karpatian to the Badenian, the sediment surfaces from the Sarmatian are less influenced by fault systems. This geometric change demonstrates the cease of synsedimentary faulting and related growth strata in the study area. According to Arzmüller *et al.* (2006), the Vienna pull-apart structures are filled mainly with upper Karpatian and Badenian sediments, which are blanketed by Sarmatian and Pannonian successions without major depositional breaks (Fig. 10).

The area of Sarmatian sedimentation and subsidence shifts to the Schwechat depression along the N-S trending Leopoldsdorf fault, and this continues until Pannonian times. This corresponds to the E-W trending extensional subsidence during the Sarmatian - Pannonian (late Middle - Late Miocene) described in the northern and central parts of the Vienna Basin (Lee and Wagreich, 2017). During late Pannonian times, several minor depocenters and subsiding areas are found in the study area; some of them are located at/near the positions of Quaternary basins (Fig. 10). Because

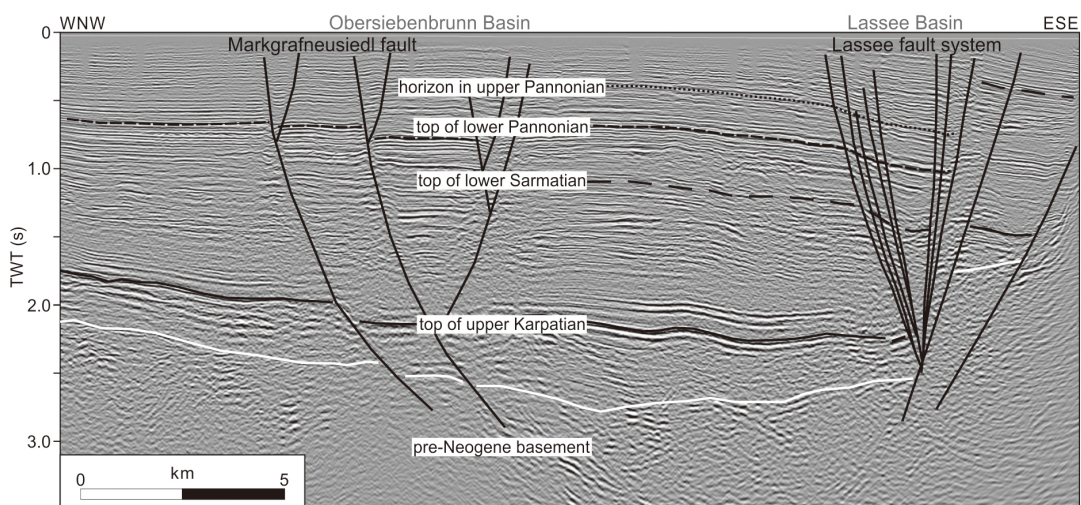


Fig. 10. A seismic section through the study area (see Figure 1c for location; revised from Beidinger and Decker, 2011). Quaternary basins (Obersiebenbrunn Basin, Lassees Basin) are overlying the Markgrafneusiedl fault and the negative flower structure of Lassees fault system.

Quaternary deposits have not been separated consistently from the Pannonian sediments in well data (Lee and Wagreich, 2016), the areas are possibly related to Quaternary subsidence (300 - 500 m/Ma in tectonic subsidence rate; Lee and Wagreich, 2017).

This case study presents the Early to Late Miocene basin evolution of the study area, successively and dimensionally in time and space. The results demonstrate that the basin evolution of the southern Vienna Basin is strongly coupled with changes of the regional paleostress regime and structural setting (especially, faults and depressions). Comparing our results to previously published studies conducted in the Vienna Basin (e.g., Jiříček and Seifert, 1990; Lankreijer *et al.*, 1995; Arzmüller *et al.*, 2006; Hölzel *et al.*, 2008; Lee and Wagreich, 2016), they match mostly those of preceding works but provide partly different models. For better understanding of the basin evolution in the Vienna Basin, the differences need to be analyzed in the further studies. However, the previous works differ in some of their methodological details. They used largely the same Central Paratethys chronostratigraphy and local zones, however without recent age refinements (e.g., Hohenegger *et al.*, 2014; Harzhauser *et al.*, 2018, in press). Additionally, in the subsidence analysis, they did not use compaction trend estimated from onsite data, but empirical porosity-depth relation from literatures for specific lithologies. And some previous studies focused only on the pull-apart evolution or part of Miocene succession, which excluded the subsidence effect by compaction of underlying sediments. Although the time factor and compacted depth are the most influential parameters in basin modelling, there are methodological differences between studies. To avoid this methodological issue and understand the basin evolution comprehensively, a basin-scale evolution modelling of the Vienna Basin is being prepared.

6. Conclusions

This study applies various analysis techniques to a case study on the Vienna Basin to introduce the basin modelling using BasinVis 2.0. The 3D basement surface model, 2D/3D sedimentation setting model and 2D/3D subsidence evolution model in seven successive stages during the Miocene are visualized in the study area and analyzed to understand the internal setting and basin evolution of the Miocene pull-apart structure in the southern part of the Vienna Basin. The results show that the basin evolution was strongly coupled with changes of the regional paleostress regime and structural setting. They match closely results of preceding works but provide partly different models, which are the basis of further studies in the Vienna Basin. This case study demonstrates that the functions and techniques of BasinVis 2.0 are effective to understand the sedimentation setting, subsidence and structural geometric evolution throughout basin history and applicable to the basin modelling.

Acknowledgement

This research was supported by Korea Research Fellowship program funded by the Ministry of Science and ICT through the National Research Foundation of Korea (2017H1D3A1A01054745) and a part of the project titled 'International Ocean Discovery Program (IODP)' funded by the Ministry of Oceans and Fisheries, Korea. Special thanks go to two reviewers for their constructive comments and Johannes Novotny, a co-developer of BasinVis 2.0, for his excellent skills and knowledge in scientific visualization.

REFERENCES

Allen, P.A. and Allen, J.R., 2013, Basin Analysis: Principles and Application to Petroleum Play Assessment, 3rd ed.

- Wiley-Blackwell, Oxford, 642 p.
- Arzmüller, G., Buchta, S., Ralbovský, E. and Wessely, G., 2006, The Vienna Basin. In: Golonka, J. and Picha, F.J. (eds.), AAPG Memoir 84: The Carpathians and Their Foreland: Geology and Hydrocarbon Resources. AAPG, Tulsa, 191-204.
- Athy, L.F., 1930, Density, porosity, and compaction of sedimentary rocks. AAPG Bulletin, 14, 1-24.
- Beidinger, A. and Decker, K., 2011, 3D geometry and kinematics of the Lasseer flower structure: Implications for segmentation and seismotectonics of the Vienna Basin strike-slip fault, Austria. Tectonophysics, 499, 22-40.
- Beidinger, A. and Decker, K., 2014, Quantifying Early Miocene in-sequence and out-of-sequence thrusting at the Alpine-Carpathian junction. Tectonics, 33, 222-252.
- Bond, G.C. and Kominz, M.A., 1984, Construction of tectonic subsidence curves for the early Paleozoic miogeocline, southern Canadian rocky mountains: implications for subsidence mechanisms, age of breakup, and crustal thinning. Geological Society of America Bulletin, 95, 155-173.
- Cressie, N., 1988, Spatial prediction and ordinary kriging. Mathematical Geology, 20, 405-421.
- Cressie, N., 1993, Spatial prediction and kriging. In: Cressie, N. (eds.), Statistics for spatial data. Wiley, New York, 105-211.
- Csontos, L., Nagymarosy, A., Horváth, F. and Kováč, M., 1992, Tertiary evolution of the Intra-Carpathian area: a model. Tectonophysics, 208, 221-241.
- Decker, K., 1996, Miocene tectonics at the Alpine-Carpathian junction and the evolution of the Vienna Basin. Mitteilungen der Gesellschaft der Geologie- und Bergbaustudenten, 41, 33-44.
- Decker, K. and Peresson, H., 1996, Tertiary kinematics in the Alpine-Carpathian-Pannonian system: links between thrusting, transform faulting and crustal extension. In: Wessely, G. and Liebl, W. (eds.), EAGE Special Publication 5: Oil and Gas in Alpidic Thrustbelts and Basins of Central and Eastern Europe. The Geological Society, London, 69-77.
- Decker, K., Peresson, H. and Hinsch, R., 2005, Active tectonics and Quaternary basin formation along the Vienna Basin Transform fault. Quaternary Science Reviews, 24, 307-322.
- Einsele, G., 2000, Sedimentary basins. Evolution, facies, and sediment budget. Springer, Berlin, 792 p.
- Fodor, L., 1995, From transpression to transtension: Oligocene-Miocene structural evolution of the Vienna basin and the East Alpine-Western Carpathian junction. Tectonophysics, 242, 151-182.
- Gardner, G.H.F., Gardner, L.W. and Gregory, A.R., 1974, Formation velocity and density-the diagnostic basics for stratigraphic traps. Geophysics, 39, 770-780.
- Haq, B.U., Hardenbol, J. and Vail, P.R., 1987, Chronology of fluctuating sea levels since the Triassic. Science, 235, 1156-1167.
- Harzhauser, M., Mandic, O., Kranner, M., Lukeneder, P., Kern, A.K., Gross, M., Carnevale, G. and Jaweck, C., 2018, The Sarmatian/Pannonian boundary at the western margin of the Vienna Basin (City of Vienna, Austria). Austrian Journal of Earth Sciences, 111, 1-26.
- Harzhauser, M., Theobalt, D., Strauss, P., Mandic, O. and Piller, W.E., in press, Seismic-based lower and middle Miocene stratigraphy in the northwestern Vienna Basin (Austria). Newsletters on Stratigraphy.
- Hinsch, R., Decker, K. and Peresson, H., 2005, 3-D seismic interpretation and structural modeling in the Vienna Basin: implications for Miocene to recent kinematics. Austrian Journal of Earth Sciences, 97, 38-50.
- Hohenegger, J., Čorić, S. and Wagneich, M., 2014, Timing of the Middle Miocene Badenian Stage of the Central Paratethys. Geologica Carpathica, 65, 55-66.
- Hölzel, M., 2009, Quantification of tectonic movement in the Vienna Basin. Ph.D. thesis, University of Vienna, Vienna, Austria, 136 p.
- Hölzel, M., Decker, K., Zámolyi, A., Strauss, P. and Wagneich, M., 2010, Lower Miocene structural evolution of the central Vienna Basin (Austria). Marine and Petroleum Geology, 27, 666-681.
- Hölzel, M., Wagneich, M., Faber, R. and Strauss, P., 2008, Regional subsidence analysis in the Vienna Basin (Austria). Austrian Journal of Earth Sciences, 101, 88-98.
- Horváth, F., 1993, Towards a mechanical model for the formation of the Pannonian basin. Tectonophysics, 226, 333-357.
- Huisman, R.S., Podladchikov, Y.Y. and Cloetingh, S., 2001, Dynamic modelling of the transition from passive to active rifting, application to the Pannonian Basin. Tectonics, 20, 1021-1039.
- Jiříček, R. and Seifert, P., 1990, Paleogeography of the Neogene in the Vienna basin and the adjacent part of the foredeep. In: Minaříková, D. and Lobitzer, H. (eds.), Thirty Years of Geological Cooperation between Austria and Czechoslovakia. Geological Survey, Prague, 89-105.
- Kováč, M., Baráth, I., Harzhauser, M., Hlavatý, I. and Hudáčková, N., 2004, Miocene depositional systems and sequence stratigraphy of the Vienna Basin. CFS Courier Forschungsinstitut Senckenberg, 246, 187-212.
- Lankreijer, A., Kováč, M., Cloetingh, S., Pitoňák, P., Hlůška, P. and Biermann, C., 1995, Quantitative subsidence analysis and forward modelling of the Vienna and Danube basins: thin-skinned versus thickskinned extension. Tectonophysics, 252, 433-451.
- Lee, E.Y., Novotny, J. and Wagneich, M., 2016, BasinVis 1.0: A MATLAB®-based program for sedimentary basin subsidence analysis and visualization. Computers & Geosciences, 91, 119-127.
- Lee, E.Y., Novotny, J. and Wagneich, M., 2019, Subsidence analysis and visualization for sedimentary basin analysis and modelling. Springer, Cham, 56 p.

- Lee, E.Y. and Wagreich, M., 2016, 3D visualization of the sedimentary fill and subsidence evolution in the northern and central Vienna Basin (Miocene). *Austrian Journal of Earth Sciences*, 109, 241-251.
- Lee, E.Y. and Wagreich, M., 2017, Polyphase tectonic subsidence evolution of the Vienna Basin inferred from quantitative subsidence analysis of the northern and central parts. *International Journal of Earth Sciences*, 106, 687-705.
- Leeder, M., 2011, *Sedimentology and sedimentary basins: from turbulence to tectonics*. Wiley, Chichester, 784 p.
- Li, J. and Heap, A., 2008, A review of spatial interpolation methods for environmental scientists. *Geoscience Australia Record 2008/23*, Canberra, 137 p.
- Mann, P., Hempton, M.R., Bradley, D.C. and Burke, K., 1983, Development of pull-apart basins. *Journal of Geology*, 91, 529-554.
- Miall, A.D., 2000, *Principles of sedimentary basin analysis*. Springer, Berlin, 616 p.
- Ori, G.G. and Friend, P.F., 1984, Sedimentary basins formed and carried piggyback on active thrust sheets. *Geology*, 12, 475-478.
- Peresson, H. and Decker, K., 1997a, Far-field effects of Late Miocene subduction in the Eastern Carpatians: E-W compression and inversion of structures in the Alpine-Carpathian-Pannonian region. *Tectonics*, 16, 38-56.
- Peresson, H. and Decker, K., 1997b, The Tertiary dynamics of the northern Eastern Alps (Austria): changing palaeostresses in a collisional plate boundary. *Tectonophysics*, 272, 125-157.
- Piller, W.E., Harzhauser, M. and Mandic, O., 2007, Miocene Central Paratethys stratigraphy - current status and future directions. *Stratigraphy*, 4, 151-168.
- Plašienka, D., Grecula, P., Putiš, M., Kováč, M. and Hovorka, D., 1997, Evolution and structure of the Western Carpatians: an overview. In: Grecula, P., Hovorka, D. and Putiš, M. (eds.), *Geological evolution of the Western Carpatians*. Mineralia Slovaca - Monograph, Bratislava, 1-24.
- Ratschbacher, L., Frisch, W. and Linzer, H.-G., 1991a, Lateral extrusion in the eastern Alps, part II: structural analysis. *Tectonics*, 10, 257-271.
- Ratschbacher, L., Merle, O., Davy, P. and Cobbold, P., 1991b, Lateral extrusion in the eastern Alps, part I: boundary conditions and experiments scaled for gravity. *Tectonics*, 10, 245-256.
- Royden, L.H., 1985, The Vienna Basin: A thin-skinned pull-apart basin. In: Biddle, K.T. and Christie-Blick, N. (eds.), *SEPM Special Publication 37: Strike-slip deformation, Basin formation and Sedimentation*. SEPM, Tulsa, 319-338.
- Royden, L.H., 1988, Late Cenozoic tectonics of the Pannonian basin system. In: Royden, L.H. and Horváth, F. (eds.), *AAPG Memoir 45: The Pannonian Basin. A study in Basin evolution*. AAPG, Tulsa, 27-48.
- Royden, L.H., Horváth, F., Nagymarosy, A. and Stegena, L., 1983a, Evolution of the Pannonian Basin System: 2. Subsidence and thermal history. *Tectonics*, 2, 91-137.
- Royden, L.H., Horváth, F. and Rumpfer, J., 1983b, Evolution of the Pannonian Basin System: 1. Tectonics. *Tectonics*, 2, 63-90.
- Salcher, B.C., Meurers, B., Smit, J., Decker, K., Hölzel, M. and Wagreich, M., 2012, Strike-slip tectonics and Quaternary basin formation along the Vienna Basin fault system inferred from Bouguer gravity derivatives. *Tectonics*, 31, TC3004, doi:10.1029/2011TC002979.
- Sauer, R., Seifert, P. and Wessely, G., 1992, Part I: Outline of Sedimentation, Tectonic Framework and Hydrocarbon Occurrence in Eastern Lower Austria. *Mitteilungen der Österreichischen Geologischen Gesellschaft*, 85, 5-96.
- Sclater, J.G. and Christie, P.A.F., 1980, Continental stretching: An explanation of the Post-Mid-Cretaceous subsidence of the central North Sea Basin. *Journal of Geophysical Research*, 85, 3711-3739.
- Steckler, M.S. and Watts, A.B., 1978, Subsidence of the Atlantic-type continental margin off New York. *Earth and Planetary Science Letters*, 41, 1-13.
- Steininger, F.F. and Wessely, G., 1999, From the Tethyan Ocean to the Paratethys Sea: Oligocene to Neogene Stratigraphy, Paleogeography and Palaeobiogeography of the circum-Mediterranean region and the Oligocene to Neogene Basin evolution in Austria. *Mitteilungen der Österreichischen Geologischen Gesellschaft*, 92, 95-116.
- Strauss, P., Harzhauser, M., Hinsch, R. and Wagreich, M., 2006, Sequence stratigraphy in a classic pull-apart basin (Neogene, Vienna Basin) - A 3D seismic based integrated approach. *Geologica Carpathica*, 57, 185-197.
- Wagreich, M. and Schmid, H.P., 2002, Backstripping dip-slip fault histories: apparent slip rates for the Miocene of the Vienna Basin. *Terra Nova*, 14, 163-168.
- Watts, A.B. and Ryan, W.B.F., 1976, Flexure of the lithosphere and continental margin basins. *Tectonophysics*, 36, 25-44.
- Watts, A.B. and Steckler, M.S., 1979, Subsidence and eustasy at the continental margin of Eastern North America. *AGU, Maurice Ewing Symposium Series*, 3, 218-234.
- Wessely, G., Kröll, A., Jiříček, R. and Nemeč, F., 1993, Wiener Becken und angrenzende Gebiete-Geologische Einheiten des präneogenen Beckenuntergrundes. *Geologische Themenkarte der Republik Österreich 1:200.000*, Geologische Bundesanstalt, Vienna.
- Xie, X. and Heller, P.L., 2009, Plate tectonics and basin subsidence history. *Geological Society of America Bulletin*, 121, 55-64.

Received : October 31, 2018

Revised : December 11, 2018

Accepted : December 12, 2018